CHAPTER 6

RELATIVISTIC MULTIREFERENCE PERTURBATION THEORY: COMPLETE ACTIVE-SPACE SECOND-ORDER PERTURBATION THEORY (CASPT2) WITH THE FOUR-COMPONENT DIRAC HAMILTONIAN

MINORI ABE[1]*, GEETHA GOPAKMAR[2], TAKAHITO NAKAJIMA[2], AND KIMIHIKO HIRAO[2]

[1]*Department of Chemistry, Graduate School of Science, Tokyo Metropolitan University, 1-1 Minami-Osawa, Hachioji-shi, Tokyo, Japan 192-0397*
[2]*Department of Applied Chemistry, School of Engineering, The University of Tokyo, Tokyo, Japan 113-8656*

Abstract: The relativistic complete active-space second-order perturbation theory (CASPT2) developed for the four-component relativistic Hamiltonian is introduced in this chapter. This method can describe the near-degenerated and dissociated electronic states of molecules involving heavy elements. This method is applicable for the systems which can be described by neither DFT nor single reference methods, and the system with very heavy-elements which cannot be described by quasi-relativistic approaches. The present theory provides accurate descriptions of bonding or dissociation states and of ground and excited states in a well-balanced way. In this review, for example, the ground and low-lying excited states of diatomic molecules with 6p series, TlH, Tl_2, PbH, and Pb_2 are calculated with the Dirac–Coulomb (DC) CASPT2 method and their spectroscopic constants and potential energy curves are presented. The obtained spectroscopic constants are compared with experimental findings and previous theoretical works. For all the molecules, the spectroscopic constants of DC-CASPT2 show reasonably good agreement with the experimental or previous theoretical spectroscopic constants

Keywords: Relativity, Four-Component, Electron Correlation, Multireference Perturbation Theory, CASPT2

* Corresponding author, e-mail: minoria@tmu.ac.jp

M. K. Shukla, J. Leszczynski (eds.), Radiation Induced Molecular Phenomena in Nucleic Acids, 157–177.

6.1. INTRODUCTION

For the computational investigation of molecular systems containing heavy atoms, such as transition metals, lanthanides, and actinides, we could neglect neither relativity nor electron correlation. Relativistic effects, both spin-free and spin-orbit, increase with the nuclear charge of atoms. Therefore, instead of the nonrelativistic Schrödinger equation, we must start with the Dirac equation, which has four-component solutions. For many-electron systems, the four-component Hamiltonian is constructed from the one-electron Dirac operator with an approximated relativistic two-electron operator, such as the Coulomb, Breit, or Gaunt operator, within the no-pair approximation. The four-component method is relativistically rigorous, which includes both spin-free and spin-orbit effects in a balanced way. However it requires much computational time since it contains more variational parameters than the approximated, one or two-component method.

So far, to overcome the time consuming defect of the four-component method, we have developed an efficient relativistic four-component polyatomic program REL4D [1], as a relativistic part of program package UTChem [2]. One important feature of REL4D is adoption of two-component Gaussian spinor with general contraction scheme for basis functions. This is not likely to the other four-component programs such as MOLFDIR [3] or DIRAC [4], and the adoption ensures more explicit kinetic balance relationship. Furthermore, the size of basis sets is also reduced compared to using decoupled scalar spin orbital basis which is used in MOLFDIR and DIRAC. The compactness of basis sets is quite efficient especially in the time-consuming parts such as two-electron integral evaluation [5] or molecular spinor integral transformation [6]. In the released version of REL4D in 2004, Dirac-Coulomb (DC) Hartree-Fock (HF), DC Kohn-Sham, and single reference electron correlation methods, such as Møller–Plesset second-order perturbation theory (MP2) are incorporated.

However, the systems with open shell d or f electrons tend to be near degenerated and single reference methods often do not work well. Instead, multireference electron correlation methods based on the four-component relativistic Hamiltonian become essential for the systems with heavy elements. Several multireference methods based on the four-component Hamiltonian had been developed previously: the Fock-space coupled cluster method by Visscher et al. [7], the configuration interaction (CI) method of Fleig et al. with the Kramers restricted MCSCF wave function [8], the generalized multiconfigurational quasi-degenerate perturbation theory (GMCQDPT) developed by Miyajima et al. [9] More recently, the complete active-space second-order perturbation theory (CASPT2) based on the four-component Dirac-Coulomb (DC) Hamiltonian was developed by ourselves [10].

The non-relativistic CASPT2 method developed by Anderson et al. [11, 12] is one of the most familiar multireference approaches. It is well established and has been applied to a large number of molecular systems with the non- or quasi-relativistic approaches. Because the CASPT2 method treats dynamic correlation effects perturbatively, it is less expensive than the multireference CI (MRCI) method. The

inexpensiveness of the CASPT2 method allows us to handle a larger number of active orbitals for correlation than the MRCI method. Molecules containing heavy-element atoms often have many degenerated valence orbitals and the number of determinants in the reference space tends to be large. This situation is undesirable for the MRCI method, because the cost of MRCI drastically increases when the dimensionality of the active space increases. If one handles a larger active space in the MRCI method, one must often decrease the dimensionality of correlated core or virtual space. Moreover, in the relativistic case, spin symmetry is not available, and the correlation calculations become more expensive than for the nonrelativistic case.

The present chapter aims to introduce the DC-CASPT2 method. Theoretical review of the four-component DC method, especially the way of taking two-component basis set in REL4D, is described in Section 6.2. and theoretical review of DC-CASPT2 is described in Section 6.3. Applications of the DC-CASPT2 method for TlH, Tl_2, PbH, and Pb_2 molecules are discussed with their potential curves in Section 6.4. Conclusions are described in the final Section, 6.5.

6.2. DIRAC-COULOMB HAMILTONIAN AND TWO-COMPONENT BASIS SPINORS

Within the Born–Oppenheimer approximation, the total electronic Dirac-Coulomb Hamiltonian is written as

$$\hat{H}_{DC} = \sum_{\lambda}^{N^{elec}} \hat{h}_D(\lambda) + \sum_{\lambda<\mu}^{N^{elec}} \hat{g}_{\lambda\mu}\,, \tag{6-1}$$

where

$$\hat{h}_D(\lambda) = c\boldsymbol{\alpha}\cdot\mathbf{p}_\lambda + (\boldsymbol{\beta}-1)c^2 - V^{nuc}(\lambda), \tag{6-2}$$

and

$$\hat{g}_{\lambda\mu}^{Coulomb} = \frac{1}{|\mathbf{r}_\lambda - \mathbf{r}_\mu|}. \tag{6-3}$$

Here, $\hat{h}_D(\lambda)$ and $\hat{g}_{\lambda\mu}^{Coulomb}$ are one- and two-electron operators, respectively. $\boldsymbol{\alpha}$ and $\boldsymbol{\beta}$ are Pauli matrices, c is the speed of light, N_{elec} is number of electrons, and $V^{nuc}(\lambda)$ is the nuclear attraction potential. The electron–electron repulsion is assumed to be the Coulomb interaction and electron-positron interactions are disregarded with no pair approximation.

As an approach analogous of nonrelativistic Hartree-Fock theory, the four-component Dirac-Hartree-Fock wave function is described with a Slater determinant of one-electron molecular functions $\{\psi_i(\mathbf{r}_\lambda),\ i = 1, \ldots, N^{elec}\}$,

$$\Psi_{HF}(\mathbf{r}_1, \mathbf{r}_2, \ldots, \mathbf{r}_{N^{elec}}) = (N^{elec}!)^{-1/2} \left| \psi_1(\mathbf{r}_1)\psi_2(\mathbf{r}_2) \ldots \ \psi_{N^{elec}}(\mathbf{r}_{N^{elec}}) \right|. \tag{6-4}$$

In the four-component case, a one-electron molecular function is not a scalar function, but a four-component vector called molecular spinor.

$$\psi_i = \begin{pmatrix} \psi_i^{2L} \\ \psi_i^{2S} \end{pmatrix} = \begin{pmatrix} \psi_{1i}^{L} \\ \psi_{2i}^{L} \\ \psi_{3i}^{S} \\ \psi_{4i}^{L} \end{pmatrix}. \tag{6-5}$$

The upper two-component vector ψ_i^{2L} is called the large-component spinor, and the lower ψ_i^{2S} is the small-component spinor. In the REL4D program, we use two-component (large- and small-component) atomic spinors (φ_p^{2L} and φ_p^{2S}) for basis set expansion.

$$\psi_i = \begin{pmatrix} \psi_i^{2L} \\ \psi_i^{2S} \end{pmatrix} = \sum_p^n \begin{pmatrix} C_{pi}^{L} \ \varphi_p^{2L} \\ C_{pi}^{S} \ \varphi_p^{2S} \end{pmatrix}. \tag{6-6}$$

Each component of φ_p^{2L} and φ_p^{2S} is generally contracted with Gaussian type spherical harmonics functions. Contraction coefficients of the basis sets are determined by four-component atomic calculations [5].

On the other hand, in the pioneering DHF and post-DHF program package MOLFDIR [3] and the well-developed four-component relativistic program package DIRAC [4], the molecular four-component spinors are expanded into decoupled scalar spin orbitals

$$\psi_i = \sum_\mu^{n^L} c_{\mu i}^{L\alpha} \varphi_\mu^{L\alpha} \begin{pmatrix} 1 \\ 0 \\ 0 \\ 0 \end{pmatrix} + \sum_\mu^{n^L} c_{\mu i}^{L\beta} \varphi_\mu^{L\beta} \begin{pmatrix} 0 \\ 1 \\ 0 \\ 0 \end{pmatrix} + \sum_\mu^{n^S} c_{\mu i}^{S\alpha} \varphi_\mu^{S\alpha} \begin{pmatrix} 0 \\ 0 \\ 1 \\ 0 \end{pmatrix} + \sum_\mu^{n^S} c_{\mu i}^{S\beta} \varphi_\mu^{S\beta} \begin{pmatrix} 0 \\ 0 \\ 0 \\ 1 \end{pmatrix}, \tag{6-7}$$

with $2n^L$ large-component and $2n^S$ small-component basis spinors. The scalar basis functions of φ^L and φ^S must obey a kinetic balance relationship,

$$\varphi_p^S = i(\boldsymbol{\sigma} \cdot \mathbf{p})\varphi_p^L \tag{6-8}$$

to avoid variational collapse. Note that this relationship only satisfies with non-relativistic atomic limit and is valid for primitive basis functions. Because of the derivative operator in this condition, the number of basis set for small component is almost twice larger than the number of basis set for large component, that is $n^S \cong 2n^L$.

The two-component basis spinors φ_p^{2L} and φ_p^{2S} in REL4D, on the other hand, obey more explicit kinetic balance relationship,

$$\varphi_p^{2S} = i(V - E - 2c^2)^{-1}(\boldsymbol{\sigma} \cdot \mathbf{p})\varphi_p^{2L}, \tag{6-9}$$

Table 6-1. Wall times in seconds for computing ERI of Au_2 with [19s14p10d5f]/(6s4p3d1f)

Program	MOLFDIR	REL4D-A[a]	REL4D–B[b]
The number of basis function			
Large components	160	160	160
Small components	420	160	160
Wall time	274864	22458	6670

[a] REL4D-A– separate contraction coefficients for quantum number a = ±;
[b] REL4D-B – same contraction coefficients for quantum number a = ±.

which completely reproduces relativistic atomic limit and is valid for contracted basis functions. The molecular spinor coefficients C_{pi}^{L} and C_{pi}^{S} are optimized commonly among the α and β components of each large or small component. Therefore the number of basis sets of large and small component is equal. If one uses the same number of large-component basis sets in the two- and one-component basis set expansion approaches, to realize same quality calculations, the two-component basis set scheme requires almost two-thirds number of basis sets of the one-component scheme. The compactness of basis sets is quite efficient, especially in the routines which depend on higher order of basis set, such as two-electron integral evaluation or molecular spinor integral transformation. For example, Au_2 system, REL4D is more than ten times faster for computing electron repulsion integral, and eight times faster for computing molecular spinor integral transformation than MOLFDIR as referred in Tables 6-1 and 6-2 [5, 6].

6.3. DIRAC-COULOMB CASPT2 METHOD

The formulation of the relativistic CASPT2 method is almost the same as the nonrelativistic CASPT2 in the second quantized form. In this section, firstly we express the relativistic Hamiltonian in the second quantized form, and then, we give a summary of the CASPT2 method [11, 12].

Table 6-2. Wall times in seconds of the integral transformation by MOLFDIR, DIRAC and REL4D in the Au_2 calculation

Program	MOLFDIR	DIRAC	REL4D
The number of basis function			
Large components	160	160	160
Small components	420	422	160
Wall time	30080[a]	16691	4310

[a] This value was the interrupted result because the MOLFDIR program was suspended with some program errors.

The total electronic Hamiltonian (6.1) is rewritten in the second quantized form as

$$\hat{H} = \sum_{p\,q} h_{pq} \hat{E}_{pq} + \frac{1}{2} \sum_{p,q,r,s} (pq|rs) \left[\hat{E}_{pq} \hat{E}_{rs} - \delta_{ps} \hat{E}_{rq} \right]. \tag{6-10}$$

Here, h_{pq} is a relativistic one-electron molecular spinor integral, and $(pq|rs)$ is a two-electron molecular spinor integral written in chemist's notation. The second quantized formulation is same as the nonrelativistic one when we use an excitation operator,

$$\hat{E}_{pq} = \hat{a}_p^\dagger \hat{a}_q, (p, q \in \text{ all molecular spinors}). \tag{6-11}$$

The operator is different from the spin-averaged nonrelativistic excitation operator denoted by

$$\hat{E}_{pq} = \frac{1}{2} \left(\hat{a}_{p\alpha}^\dagger \hat{a}_{q\alpha} + \hat{a}_{p\beta}^\dagger \hat{a}_{q\beta} \right) (p, q \in \text{ all molecular orbitals}). \tag{6-12}$$

The absence of spin symmetry in the relativistic case makes the indices run over all spinor space, which is twice as wide as the non-relativistic orbital space.

Here, we summarize the CASPT2 method [11, 12]. In perturbation theory in the correlation problem, partitioning of the total Hamiltonian $\hat{H}$ into a 0th-order Hamiltonian $\hat{H}_0$ and a small perturbation $\hat{V}$ is a major problem. The 0th-order wave function $|0\rangle$, which is the eigenstate of $\hat{H}_0$, should be mostly close to the exact eigenstate of $\hat{H}$ for the rapid convergence of the perturbation. As a 0th-order wave function, the CASPT2 method adopts a multiconfigurational wave function generated from the CASSCF or CASCI calculations.

To determine $\hat{H}_0$, the configurational space for the expansion of the wave function is introduced. The space is divided into four subspaces: V_0, V_K, V_SD, and $V_\mathrm{TQ...}$. V_0 is the one-dimensional space spanned by a CASSCF or CASCI reference function $|0\rangle$. V_K is the space spanned by the orthogonal complements of $|0\rangle$, which is obtained by the same CASCI calculation that generates the reference function. V_SD is the space spanned by the single and double replacement states from the reference function, and $V_\mathrm{TQ...}$ is the space spanned by all the higher order replacement states from the reference function. Only the states in V_SD contribute to the expansion of the first-order wave function and the second-order correlation energy, because only states in V_SD interact with the reference function via the total Hamiltonian $\hat{H}$. The $\hat{H}_0$ in CASPT2 is constructed so that only V_SD contributes to the expansion of the first-order wave function. The resulting $\hat{H}_0$ is given by

$$\widehat{H}_0 = \widehat{P}_0 \widehat{F} \widehat{P}_0 + \widehat{P}_\mathrm{K} \widehat{F} \widehat{P}_\mathrm{K} + \widehat{P}_\mathrm{SD} \widehat{F} \widehat{P}_\mathrm{SD} + \widehat{P}_\mathrm{TQ...} \widehat{F} \widehat{P}_\mathrm{TQ...} \tag{6-13}$$

Here, $\widehat{P}_0$, $\widehat{P}_\mathrm{K}$, $\widehat{P}_\mathrm{SD}$, and $\widehat{P}_\mathrm{TQ...}$ denote projection operators to V_0, V_K, V_SD, and $V_\mathrm{TQ...}$ subspaces, respectively.

$\widehat{F}$ in Eq. (6-13) is a sum of one-electron operators and is given by

$$\widehat{F} = \sum_{\mathrm{pq}} f_{\mathrm{pq}} \widehat{E}_{\mathrm{pq}}. \tag{6-14}$$

Here, f_{pq} is the generalized Fock matrix elements,

$$f_{\mathrm{pq}} = h_{\mathrm{pq}} + \sum_{\mathrm{rs}} D_{\mathrm{rs}} \left[(\mathrm{pq}\,|\mathrm{rs}) - (\mathrm{ps}\,|\mathrm{rq}) \right], \tag{6-15}$$

where D_{rs} is the first-order density matrix element.

The first-order wave function, which determines the second-order correlation energy, is expanded with a set of $|i\rangle$ in V_{SD} space as

$$|\Psi_1\rangle = \sum_{i=1}^{M} C_i \,|i\rangle\,, \tag{6-16}$$

and the coefficients C_i are determined by the linear equations

$$\sum_{j=1}^{M} C_j \,\langle i|\, \widehat{H}_0 - E_0 \,|j\rangle = -\,\langle i|\, \widehat{H}\,|0\rangle\,, i = 1, \ldots..,\ M \tag{6-17}$$

where $E_0 = \langle 0|\, \widehat{H}_0\,|0\rangle$ is the 0th-order energy and M is the total number of states $|i\rangle$, which is the multiconfigurational state in V_{SD} space, $\hat{E}_{pq}\hat{E}_{rs}\,|0\rangle$.

If the one-electron operator of Eq. (6-14) consists of only diagonal operators, that is $\widehat{F} = \sum_{\mathrm{p}} f'_{\mathrm{pp}} \widehat{E}_{\mathrm{pp}}$, the linear equations of Eq. (6-17) are separated into eight noninteracting subgroups. In this case, the evaluation of the inverse matrix of $\langle i|\, \widehat{H}_0 - E_0\,|j\rangle$, which is required to solve Eq. (6-17), is also divided into eight subgroups and the cost of calculation is decreased. Therefore, to obtain the diagonal Fock operator, f_{pq} is transformed to $f'_{\mathrm{pq}} = \delta_{pq}\varepsilon_p$ by a unitary transformation with block diagonalizations within three subspaces: inactive, active, and secondary. Molecular spinors are also transformed by the unitary transformation. The transformed spinors are used as a one-electron basis to obtain the first-order wave function. After solving Eq. (6-17) within the eight subgroups, the second-order energy with the diagonal Fock operator is evaluated by

$$E_2 = \langle 0|\, \hat{H}\,|\Psi_1\rangle \tag{6-18}$$

The effects of the nondiagonal part of the Fock operator in Eq. (6-14) can be estimated additionally with an iterative procedure [12]. More details are given in refs. [11, 12].

In the relativistic CASPT2 method, the matrix elements $\langle i|\, \widehat{H}_0 - E_0\,|j\rangle$ and $\langle i|\, \widehat{H}\,|0\rangle$ are evaluated with the excitation operator in the spinor basis, rather than

the nonrelativistic spin-averaged excitation operator in the orbital basis. Thus, double-group symmetry can be used instead of the single-group treatment in the nonrelativistic approach. Consequently, in the relativistic case, the complex values of one- and two-electron integrals and CI coefficients must be handled. This makes computational cost larger than in the nonrelativistic case.

6.4. APPLICATIONS

6.4.1. Computational Details

Low-lying states of TlH, Tl_2, PbH, and Pb_2 molecules were calculated with the four-component DC-CASPT2 method. For the TlH and Tl_2 molecules, various theoretical calculations have been reported so far and readers are referred to refs. [13–16], [17–22], for TlH and Tl_2 respectively. For the PbH and Pb_2 molecules, theoretical applications are fewer, such as reference [23] for PbH and refs [19, 24] for Pb_2. In the TlH molecule, the Hartree–Fock (HF), the second-order Møller–Plesset (MP2) theory, and the complete active-space configuration interaction (CASCI) based on the DC Hamiltonian (DC-HF, DC-MP2, and DC-CASCI) were also calculated for comparison with DC-CASPT2. The DC-CASCI wave function was used as the reference function for DC-CASPT2. Molecular spinors were determined by the RHF or ROHF methods. For virtual spinors, the improved virtual orbital (IVO) method [25, 26] was adopted. Usually, CASSCF is used as the reference function of non-relativistic CASPT2. While application of four-component relativistic CASSCF is theoretically possible, analogues of Fleig's work [8], it requires complicated calculations. Instead of CASSCF, we applied the CASCI-IVO method as the reference function which is more simple and robust than CASSCF. We used DC-CASPT2 with the diagonal approximation [11] for the present calculations. The REL4D part [1] in the UTChem program package [2] was used for the DC-HF [5], integral transformation [6], and the DC-MP2 calculations. For IVO, DC-CASCI, and DC-CASPT2 calculations, new programs were developed.

Spherical harmonic Gaussian-type basis spinors with general contraction were used throughout this study. For TlH and Tl_2 calculations, the exponents of the Gaussian basis functions [27] determined by the spin-free third-order Douglas–Kroll (DK3) method [28] with point-charge nucleus model were used, and contraction coefficients were determined by the four-component atomic SCF calculation [29]. For PbH and Pb_2 calculations, relativistic Gaussian basis set with finite nucleus model determined by Faegri [30] was used. The finite nucleus model was adopted for PbH and Pb_2 calculations, whereas point-charge nucleus model was adopted for TlH and Tl_2. Outer exponents were decontracted to be valence triple-zeta quality and several diffused primitive exponents were added by even tempered method from division by 2.5. The size of the large-components basis sets is as follows; H:[8s2p]/(5s2p), Tl:[28s23p15d11f]/(10s7p6d4f) for TlH and Tl_2, H:[8s2p]/(5s2p) and Pb:[25s21p14d9f]/(10s7p5d3f) for PbH, and Pb:[25s21p14d9f]/(10s9p5d3f) for

Pb_2. Spectroscopic constants of equilibrium bond lengths (R_e), harmonic frequencies (ω_e), adiabatic transition energies (T_e), and dissociation energies (D_e) were obtained by fitting to an analytical form using cubic splines. The dissociation energy was obtained by substitution from the sum of energies of the atomic states to the minimum energy of the molecular state. To simplify notations, we abbreviate the taking of active space and active electrons in CASCI calculations to the form CASCI (N_{act}, N_{elec}). N_{act} indicates the number of spinors in the active space, and N_{elec} indicates the number of electrons in the active space. For the CASPT2 calculations, we also use abbreviations such as CASPT2(N_{inact}, N_{act}, N_{sec}) with the number of spinors in inactive space, N_{inact}, active space, N_{act}, and secondary space, N_{sec}, respectively.

6.4.2. TlH Molecule

The DC-CASCI (12, 4) calculation was performed to construct reference functions. The active space includes the molecular spinors, which have atomic nature of $6s_{1/2}$, $6p_{1/2}$, $6p_{3/2}$ of Tl and $1s_{1/2}$ of H, and two virtual molecular spinors. The DC-CASPT2 (10, 12, 110) calculation followed and this choice of active space provided smooth potential curves for four low-lying states of TlH at the DC-CASPT2 level.

The potential curves for the ground state with the DC-HF, DC-MP2, DC-CASCI, and DC-CASPT2 methods are illustrated in Figure 6-1, which shows that the deviation of the multireference methods, DC-CASCI and DC-CASPT2, from the single-reference methods, DC-HF and DC-MP2, becomes significant in the region of longer bond length. From the spectroscopic constants listed in Table 6-3 with experimental data [31], the DC-CASPT2 method provides better agreement with experiment for the three properties, R_e, ω_e, and D_e than the DC-HF, DC-CASCI, and DC-MP2 method.

In the bonding region, the ground state of DC-CASCI is mainly contributed by the DC-HF determinant and the DC-HF weight is about 97%. The static correlation of DC-CASCI provides 0.052 Å longer bond length and 190 cm^{-1} smaller harmonic frequency than the DC-HF results. The DC-CASCI results overestimate the experimental bond length and underestimate the experimental frequency. The dynamic correlation by DC-CASPT2 corrects the bond length and frequency of DC-CASCI toward the experimental values. The deviation of the DC-CASPT2 result from the experimental values ($R_e = 1.870$ Å and $\omega_e = 1391\,cm^{-1}$) is 0.023 Å in bond length and 40 cm^{-1} in harmonic frequency.

The ground state and three low-lying states calculated at the DC-CASPT2 level are shown in Figure 6-2 and assigned as 0^+(I), 0^-, 1, and 0^+(II), from the lower states respectively. In our calculation, only the 0^+(II) state has minimum energy among the excited states. This state has a dissociation channel of the $^2P_{3/2}$ excited state of Tl and the $^1S_{1/2}$ ground state of H, while the other three states have a

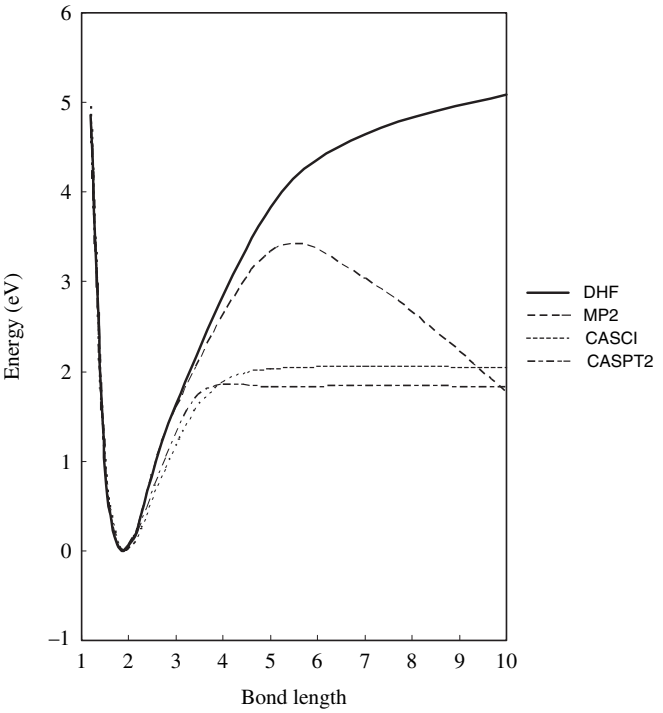

Figure 6-1. Potential energy curves of the ground state of TlH with various four-component electron correlation methods

dissociation channel of the $^2P_{1/2}$ ground state of Tl and the $^1S_{1/2}$ ground state of H. The spectroscopic constants of the 0^+(II) state are listed in Table 6-4 with experimental findings [32] and the previous theoretical work by Rakowitz et al.[15] Our DC-CASPT2 result for 0^+(II) state agrees with both experiments and the theoretical spin-orbit CI works very well.

Table 6-3. Spectroscopic constants of ground state TlH (0_g^+) at several calculation levels

Method	R_e (Å)	ω_e (cm^{-1})	D_e(eV)
Present calculations			
DC-HF	1.871	1447	–
DC-MP2	1.869	1425	–
DC-CASCI	1.923	1257	1.45
DC-CASPT2	1.893	1351	1.87
exp.[a]	1.870	1391	2.06

[a] Ref. [31].

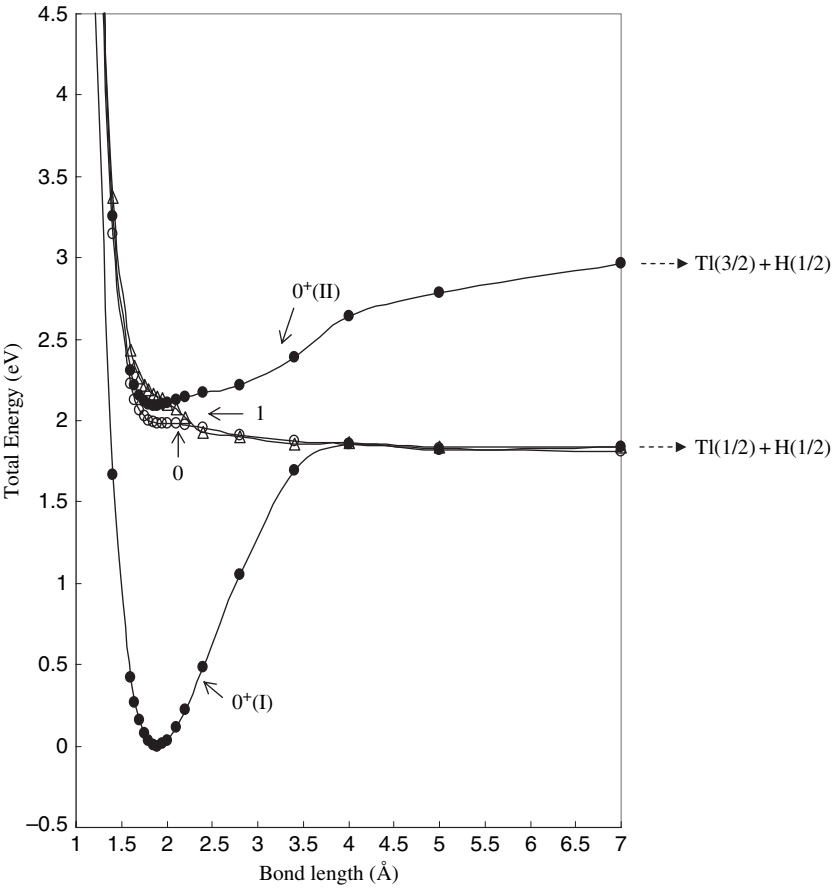

Figure 6-2. Potential energy curves of low-lying TlH states at the DC-CASPT2 level. 0^+:—○—, 0^-:---●---, 1:—△—

6.4.3. Tl_2 Molecule

The DC-CASCI (16, 2) calculation was performed to construct reference functions. The active space includes the molecular spinors, which have atomic nature of 6*p* spinors of two Tl and four virtual molecular spinors. We followed this with the DC-CASPT2 (12, 16, 128) calculation, and nine low-lying states were obtained. Potential curves of the nine low-lying states of Tl_2 calculated at the DC-CASPT2 level are shown in Figure 6-3. The spectroscopic constants of the ground state (0_u^-) at the DC-CASCI and DC-CASPT2 levels are listed in Table 6-5 with the Raman experimental data [33] and the two-component Kramers restricted (KR) CI results with relativistic effective potential (REP), reported by Kim et al. [17] and Han et al. [18], and the spin–free DK2-CASPT2 results with perturbative spin–orbit coupling

Table 6-4. Spectroscopic constants of the excited state of TlH (0_g^+(II)) at the DC-CASPT2 level with previous findings

Method	R_e (Å)	D_e(eV)	T_e(eV)
DC-CASPT2	1.861	0.85	2.09
SOCIEX[a]	1.86	–	2.07
exp.[b]	1.86	–	2.18

[a] Rakowitz et al. Spin-orbit CI with energy extrapolation [15]; [b] Ref. [32].

by Roos et al. [19] The states obtained by DC-HF and DC-MP2 methods are 0_g^+, which have different symmetry from the ground state, and hence the results of DC-HF and DC-MP2 are not included in Table 6-3. For the excited states, the DC-CASPT2 results are listed in Table 6-6 compared with the two-component KRCI method by Kim et al. [17]

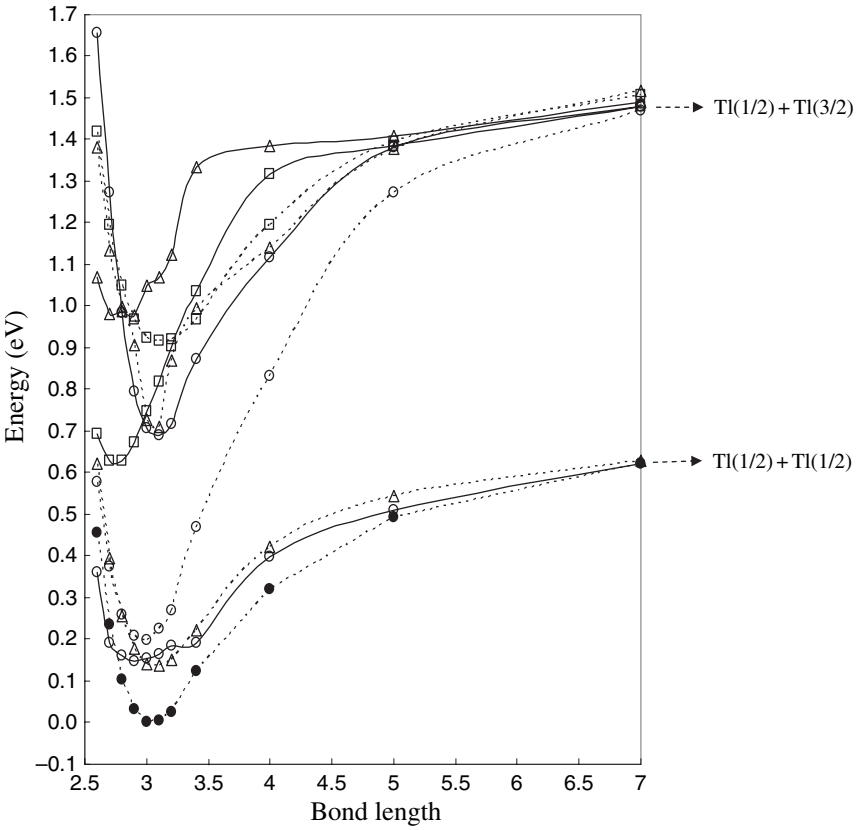

Figure 6-3. Potential energy curves of the nine low-lying states of Tl_2 at the DC-CASPT2 level. 0_g^+: ---○---, 0_u^+: ——○——, 0_u^-: ——●——, 1_g: ——△——, 1_u: ---△---, 2_g: ——□——, 2_u:---□---

Table 6-5. Spectroscopic constants of the ground state Tl_2 (0_u^-) at several calculation levels

Method	R_e (Å)	ω_e (cm^{-1})	D_e(eV)
DC-CASCI	3.56	39	–0.01
DC-CASPT2	3.04	84	0.51
KRCI-REP[a]	3.30	55	0.32
KRCI-REP[b]	3.11	75	0.34
CASPT2-SOC[c]	3.09	75	0.43
exp.[d]	3.00	78	0.43 ± 0.04

[a]Two-component KR-RASCI(ras1 = 4,ras2 = 12,ras3 = 36) with REP by Kim et al. [17]; [b]Two-component KR-RASCI(ras1 = 24,ras2 = 4,ras3 =full virtual spinors) with REP Han et al. [18]; [c]Spin–free CASPT2 with perturbative spin–orbit coupling (SOC) by Roos et al. [19]. The dissociation energy is D_0 value; [d]Ref. [33]. The dissociation energy is D_0 value.

In Table 6-3, the spectroscopic constants of the ground state (0_u^-) with DC-CASPT2 ($R_e = 3.04$ Å, $\omega_e = 84\,cm^{-1}$, and $D_e = 0.51\,eV$) show satisfactory agreement with the experimental results ($R_e = 3.0$ Å, $\omega_e = 78\,cm^{-1}$, and $D_0 = 0.43 \pm 0.03\,eV$) [33]. From the comparison to the DC-CASCI result ($R_e = 3.56$ Å, $\omega_e = 39\,cm^{-1}$, and $D_e = -0.01\,eV$), dynamic correlation by DC-CASPT2 is very important for the weak bonding description of the Tl_2 molecule. The present DC-CASPT2 method yields the similar result in comparison with the previous theoretical results. For the properties in the excited states in Table 6-4, DC-CASPT2 and KRCI by Kim et al. have relatively similar values of T_e among the lower four states, 0_u^-, 1_u(I), 0_g^+(I), and 0_u^+. Other properties, R_e, ω_e, and D_e of these states are not very similar because the CI calculation by Kim et al. uses a smaller spinor space in correlation than the present DC-CASPT2 calculation.

Table 6-6. Spectroscopic constants of the nine low-lying states of Tl_2 at the DC-CASPT2 level with previous theoretical results

	DC-CASPT2				KRCI-REP[a]			
State	R_e (Å)	ω_e (cm^{-1})	D_e (eV)	T_e (eV)	R_e (Å)	ω_e (cm^{-1})	D_e (eV)	T_e (eV)
0_u^-	3.04	84	0.51	0	3.30	55	0.32	0
1_u(I)	3.07	79	0.37	0.135	3.36	47	0.20	0.115
0_g^+(I)	2.90	79	0.36	0.146	3.62	29	0.15	0.169
0_u^+	2.97	98	1.24	0.198	3.16	73	0.90	0.232
2_g	2.74	123	0.81	0.622	3.08	62	0.17	0.973
0_g^+(II)	3.08	111	0.74	0.690	3.34	66	0.42	0.727
1_u(II)	–	–	–	(~0.7)	3.33	54	0.32	0.824
2_u	3.09	60	0.52	0.917	3.26	64	0.51	0.628
1_g	–	–	–	(~0.9)	2.96	87	0.47	0.662

[a]Two-component KR-RASCI(4, 12, 36) with REP by Kim et al. [17]

6.4.4. PbH Molecule

The DC-CASCI (10, 3) calculation was performed to construct reference functions. The active space includes the molecular spinors, which have atomic nature of $6s_{1/2}$, $6p_{1/2}$, and $6p_{3/2}$ of Pb and $1s_{1/2}$ of H and three virtual molecular spinors. This was followed with the DC-CASPT2 (26, 10, 86) level of calculation which provided smooth curves both at the bonding and dissociation regions for five of the low-lying states. These potential curves are represented in Figure 6-4. The spectroscopic constants of the lowest lying states ($\Omega = 1/2$ (ground) and $\Omega = 3/2$) at the DC-CASCI and DC-CASPT2 level of computation are compared and listed in Table 6-7 with the experimental data [34]. Theoretical calculations using the generalized relativistic effective core potential (GRECP) followed by multireference

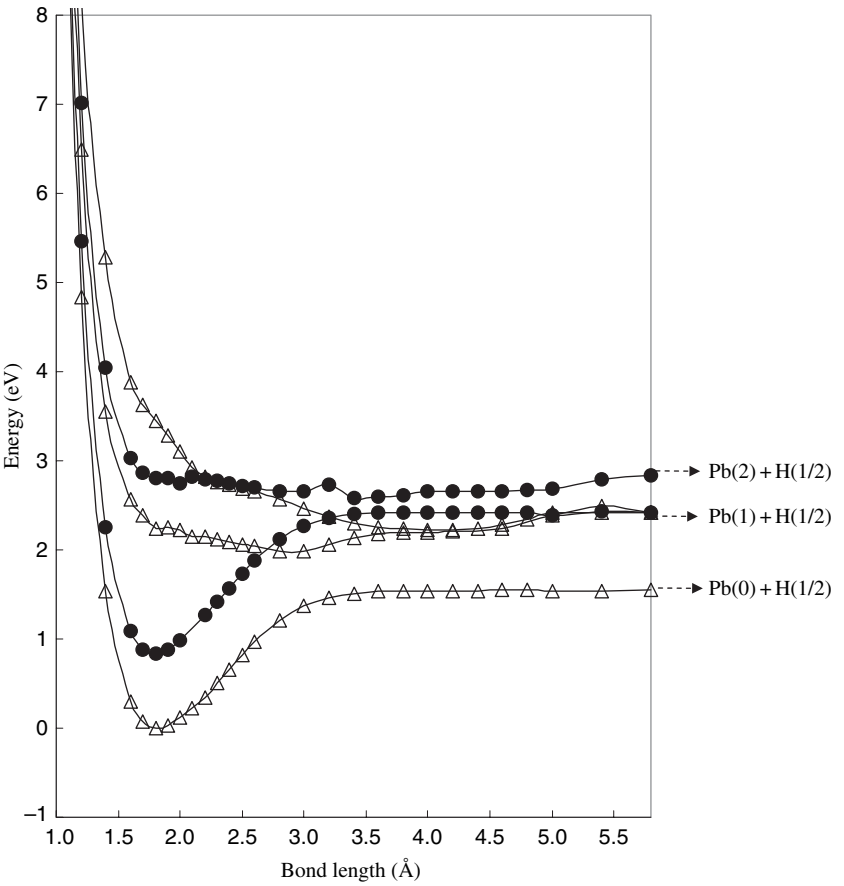

Figure 6-4. Potential energy curves of the five low-lying states of PbH at the DC-CASPT2 level. 1/2:···△···, 3/2:—●—

Table 6-7. Spectroscopic constants of the two low-lying states of PbH with experimental findings and previous calculation. BSSE is estimated by counterpoise correction (CPC)

Method	R_e (Å)	ω_e (cm^{-1})	D_e(eV)	T_e (eV)
1/2 state (ground state)				
DC-CASCI (10, 3)	1.830	1628	0.69	0
DC-CASCI (10, 3)+CPC	1.830	1627	0.87	0
DC-CASPT2 (26, 10, 86)	1.816	1601	1.39	0
DC-CASPT2 (26, 10, 86)+CPC	1.849	1514	1.42	0
GRECP/5eMRD-CI[a]	1.871	1686	1.44	0
exp.[b]	1.838	1564	≤ 1.59	0
3/2 state				
DC-CASCI (10, 3)	1.806	1708	0.80	0.805
DC-CASPT2 (26, 10, 86)	1.790	1685	1.39	0.829
GRECP/5eMRD-CI[a]	1.855	1727	–	0.797
exp.[c]	–	–	–	~ 0.855

[a]five electrons MRD-CI calculation with GRECP by Isaev et al. [23]; [b]Ref. [34]; [c]Unpublished data by Fink et al.

single- and double-excitation configuration interaction (MRD-CI) method by Isaev et al. [23] are also listed.

For the ground state, we performed counterpoise corrections (CPC) to estimate basis set superposition error (BSSE). While DC-CASPT2 without CPC provides slightly shorter bond length (0.016 Å) and larger frequency (37 cm^{-1}) than experimental values, CPC improves these values toward the experiment, longer bond length (0.011 Å) and smaller frequencies (50 cm^{-1}). The present DC-CASPT2-CPC results show good agreement with experiment. The effects of CPC are 0.033 Å in bond length, 87 cm^{-1} in harmonic frequency, and 0.03 eV in dissociation energy. For the first excited state, 3/2(I), the excitation energy of DC-CASPT2 (0.829 eV) is quite close to the experimental value ($\sim$0.855 eV). The 3/2(I) state have shorter bond length and larger harmonic frequency than the ground state and this tendency is similar to the previous calculation with GRECP/MRDCI method. Atomic spectra of Pb at the DC-CASPT2 level are also consistent with experimental values: First excitation energy, 0.830 eV, and second excitation energy, 1.278 eV, are obtained by the DC-CASPT2 method, whereas experimentally they are determined 0.970 eV and 1.320 eV respectively [35].

6.4.5. Pb_2 Molecule

The DC-CASCI (12, 4) calculation was performed to construct reference functions. The active space includes the molecular spinors, which have atomic nature of $6p_{1/2}$ and $6p_{3/2}$ of Pb. This was followed with the DC-CASPT2 (24, 12, 160) level of calculation and the potential energy curves are illustrated in Figure 6-5a. This figure includes all the states which go to the first, second, and third dissociation channels, except 1_u(II) state, which had intruder state problem. For simplification

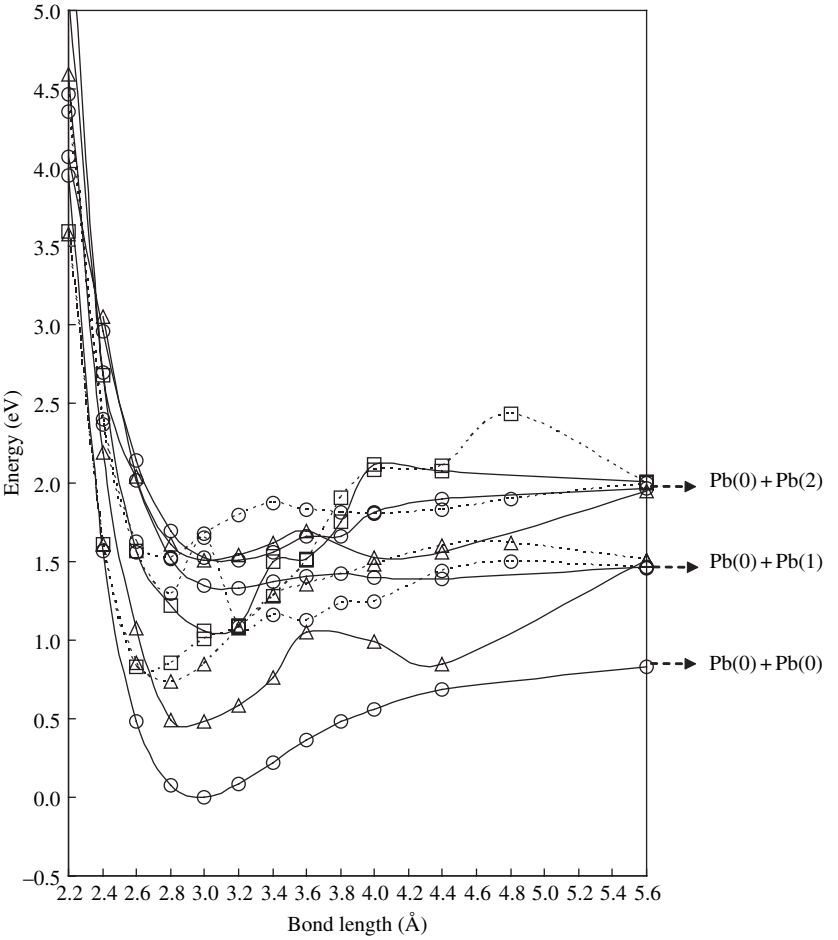

Figure 6-5a. Potential energy curves of the ten low-lying states of Pb_2 at the DC-CASPT2 level. 0_g:—○—, 0_u:---○---, 1_g:—□—, 1_u:---□---, 2_g:—△—, 2_u:---△---

of Figure 6-5ca, gerade and ungerade symmetries are separately represented in Figures 6-5cb and 6-5cc, respectively. In Table 6-8, spectroscopic constants of the ground state, 0_g, at the DC-CASPT2 with and without CPC are listed with experimental data [36, 37] and a previous theoretical work with spin–free Douglas-Kroll CASPT2 with perturbative spin–orbit coupling (SOC) by Roos et al. [19]. [25s21p14d9f]/(10s9p5d3f) basis set, triple zeta (TZ) quality with two s-type and two p-type diffuse primitive functions (TZ+2s+2p), was used to obtain the whole potential curves and spectroscopic properties of ground and excited states. To estimate the effects of BSSE for the ground state, two types of basis sets were also used, TZ with two s-type primitive functions (TZ+2s) and TZ with two s−, two

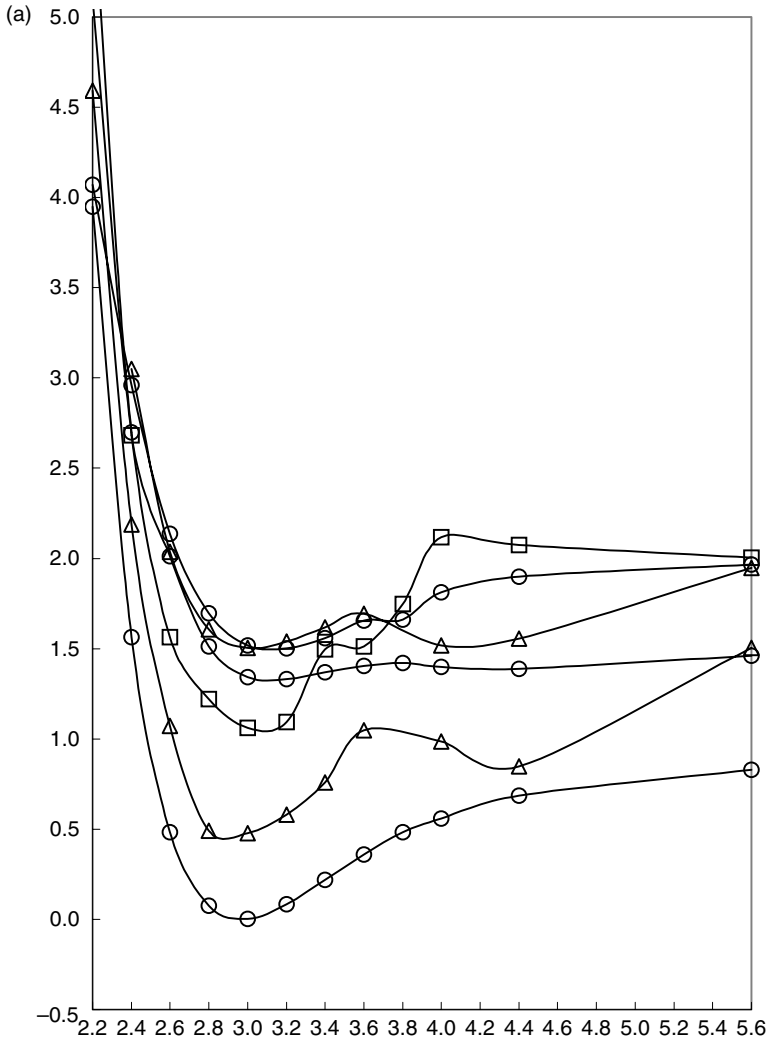

Figure 6-5b. Potential energy curves of the gerade states of Pb_2 at the DC-CASPT2 level. 0_g(I), 0_g(II), 0_g(III), 1_g(I), 1_g(II), and 2_g(I) states are included. 0_g: —○—, 1_g: —□—, 2_g: —△—

p−, and one d-type primitive functions (TZ+2s+2p+1d). Spectroscopic constants of two excited states, 0_g(III) and 1_u(I), were analyzed and listed in Table 6-9.

The ground state properties of DC-CASPT2 summarized in Table 6-8, are reasonably consistent with the experimental data and the previous calculations, except that dissociation energy was underestimated in our calculations. In the case of Pb_2, unlikely to PbH, CPC did not give improvement in all types of the basis sets, and the CPC effects are 0.034 Å in bond length, 3.4 cm^{-1} in frequency, and 0.10 eV

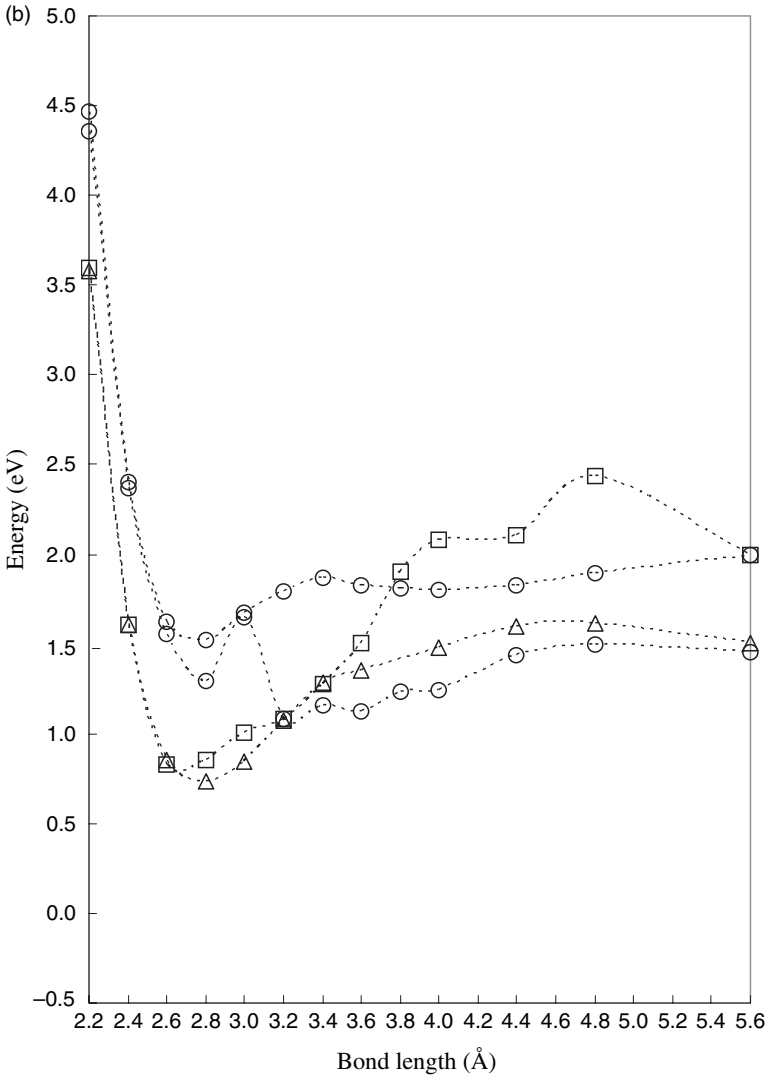

Figure 6-5c. Potential energy curves of the ungerade states of Pb_2 at the DC-CASPT2 level. 0_u(I), 0_u(II), 1_u(I), and 2_u(I) states are included. 0_u: ---⊙---, 1_u: ---⊡---, 2_u: ---△---

in dissociation energy when TZ+2s+2p basis was used. Among the three types of basis sets, the largest basis set provides closest results to the experiment and the deviations of CPC become also smallest. In this molecule, the basis-set dependency is important, and more additional functions are required not only diffuse but also polarization, for accuracy beyond the present calculations. In Figure 5a, while the ground state exists and dissociates solely, low-ling excited states are closely

Table 6-8. Spectroscopic constants of the ground state of Pb_2 (0g), with various basis sets at the DC-CASPT2 level. BSSE is estimated by counterpoise correction (CPC)

	DC-CASPT2 without CPC			DC-CASPT2 with CPC		
Basis sets[a]	R_e (Å)	ω_e (cm^{-1})	D_e(eV)	R_e (Å)	ω_e (cm^{-1})	D_e(eV)
TZ+2s	2.983	103.4	0.927	3.018	98.4	0.506
TZ+2s+2p	2.969	107.4	0.525	3.003	104.0	0.424
TZ+2s+2p+1d	2.968	109.2	0.630	3.000	106.7	0.550

Previous works	R_e (Å)	ω_e (cm^{-1})	D_e(eV)
CASPT2+SOC[a]	2.937	104	0.917
exp.	2.932[b]	110[c]	0.86[c]

[a]Spin–free CASPT2 with perturbative spin–orbit coupling (SOC) by Roos et al. [19]; [b]Ref. [36]; [c]Ref. [37]

located each other and show complex structures, like avoided crossings. The states with double minimum or pertubatively unstable were eliminated from spectroscopic calculations and 1_u(I) and 0_g(III) are analyzed . There are neither experimental nor theoretically work before for the excited state of Pb_2, and this is the first prediction for the system.

6.5. CONCLUSIONS

We have reviewed the relativistic CASPT2 method with the four-component Dirac Hamiltonian, which has been proposed by our group recently. Because of the high computational demands of relativistic multireference correlation methods, the perturbative approach of dynamic correlation in the present method provides feasible calculations and the ability to use wider correlated spinor spaces than the relativistic multireference CC or CI methods. As examples, 6*p* series diatomic molecules are calculated with the CASPT2 diagonal approximation based on CASCI-IVO reference functions. The relativistic CASPT2 method shows good agreement with

Table 6-9. Spectroscopic constants of low-lying states of Pb_2 molecule (0_g(I), 0_g(III) and 1_u(I)), at the DC-CASPT2 level. The size of basis set for Pb is [25s21p14d9f]/(10s9p5d3f)

	R_e (Å)	ω_e (cm^{-1})	D_e(eV)	T_e(eV)
0_g(I)	2.969	107.4	0.525	0
1_u(I)	2.800	184.8	0.790	0.722
0_g(III)	3.123	79.9	0.462	1.497

experimental and previous accurate ab initio calculations for the spectroscopic constants of both ground and low-lying excited states.

Because of highly accurate treatment of relativity with the four-component Dirac Hamiltonian, the present theory makes it possible to investigate molecules involving any heavy-element atoms. Since the present method is multireference-base, we can handle the systems with complicated electronic structures, for examples, lanthanide and actinide compounds, which often have a large number of near-degenerated states. Besides, unlikely to single-reference methods, the CASPT2 method can describe dissociation of bonding and effective to tract chemical reactions. Thus, it is expected that the relativistic CASPT2 will be a powerful tool to search new chemical reactions with heavy-element atoms.

REFERENCES

1. REL4D: Abe M, Iikura H, Kamiya M, Nakajima T, Yanagisawa S, Yanai T.
2. Yanai T, Kamiya M, Kawashima Y, Nakajima T, Nakano H, Nakao Y, Sekino H, Paulovic J, Tsuneda T, Yanagisawa S, Hirao K (2004) The UTChem program package is available on http://utchem.qcl.t.u-tokyo.ac.jp/
3. Visscher L, Visser O, Aerts H, Merenga H, and Nieuwpoort WC (1994) Comput Phys Commun 81: 120.
4. Saue T, Fægri K, Jr, Helgaker T, and Gropen O (1997) Mol Phys 91: 937.
5. Yanai T, Nakajima T, Ishikawa Y, and Hirao K (2001) J Chem Phys 114: 6526.
6. Abe M, Yanai T, Nakajima T, and Hirao K (2004) Chem Phys Lett 388: 68.
7. Visscher L, Eliav E, and Kaldor U (2001) J Chem Phys 115: 9720.
8. Fleig T, Jensen HJA, Olsen J, and Visscher L (2006) J Chem Phys 124: 104106.
9. Miyajima M, Watanabe Y, and Nakano H (2006) J Chem Phys 124: 044101.
10. Abe M, Nakajima T, and Hirao K (2006) J Chem Phys 125: 234110.
11. Andersson K, Malmqvist PÅ, Roos BO, Sadlej AJ, and Woliński K (1990) J Phys Chem 94: 5483.
12. Andersson K, Malmqvist PÅ, and Roos BO (1992) J Chem Phys 96: 1218.
13. Seth M, Schwerdtfeger P, and Fægri K (1999) J Chem Phys 111: 6422.
14. Fægri K and Visscher L (2005) Theor Chem Acc 105: 265.
15. Rakowitz F and Marian CM (1997) Chem Phys 225: 223.
16. Hess BA and Maran CM (2000) In: Jensen P and Bunker PR (ed) Computational Molecular Spectroscopy, Wiley, Sussex, p. 169.
17. Kim MC, Lee HS, Lee YS, and Lee SY (1998) J Chem Phys 109: 9384.
18. Han YK and Hirao K (2000) J Chem Phys 112: 9353.
19. Roos BO and Malmqvist PÅ (2004) Phys Chem Chem Phys 6: 2919.
20. Christiansen PA (1983) J Chem Phys 79: 2928.
21. Christiansen PA and Pitzer KS (1981) J Chem Phys 74: 1162.
22. Vijayakumar M and Balasubramanian K (1992) J Chem Phys 97: 7474.
23. Isaev TA, Mosyagin NS, Titov AV, Alekseyev AB, and Buenker RJ (2002) Int J Quantum Chem 88: 687.
24. Mayer M, Kruger S, and Rosch N (2001) J Chem Phys 115: 4411.
25. Huzinaga S and Arnau C (1970) Phys Rev A 1: 1285.
26. Potts DM, Taylor CM, Chaudhuri RK, and Freed KF (2001) J Chem Phys 114: 2592.
27. Tsuchiya T, Abe M, Nakajima T, and Hirao K (2001) J Chem Phys 115: 4463.
28. Nakajima T and Hirao K (2000) J Chem Phys 113: 7786.

29. Koc K and Ishikawa Y (1994) Phys Rev A 49: 794.
30. Faegri K (2001) Theo Chem Acc 105: 252.
31. Huber KP and Hertzberg G (1979) In: Molecular Spectra and Molecular Structure. IV. Constants of diatomic molecules, van Nostrand Reinhold, New York.
32. Ginter ML and Battino R (1965) J Chem Phys 42: 3222.
33. Froben FW, Schulze W, and Kloss U (1983) Chem Phys Lett 99: 500.
34. Hertzberg (1950) In: Molecular spectra and Molecular structure. I. Spectra of Diatomic Molecules, Van Nostrand Reinhold, New York.
35. Wood D and Andrew KL (1968) J Opt Soc Am 58: 818.
36. Frohen F, Schulze W, and Kloss U (1983) Chem Phys Letters 99: 500.
37. Sonntag H and Weber R (1983) J Mol Spectrosc 100: 75.